Bioorganic & Medicinal Chemistry Letters 28 (2018) 2837–2841

Contents lists available at ScienceDirect

Bioorganic & Medicinal Chemistry Letters

journal homepage: www.elsevier.com/locate/bmcl

Discovery of small molecule inhibitors of adenovirus by disrupting E3-19K/HLA-A2 interactions

Jinhong Ren[a,1], Nikita R. Dsouza[b,1], Hui Deng[c], Hyun Lee[a,d,e], Marlene Bouvier[c], Michael E. Johnson[a,b,d,*]

[a] Center for Biomolecular Sciences, University of Illinois at Chicago, 900 S. Ashland Ave, Chicago, IL 60607, USA
[b] Department of Bioengineering, University of Illinois at Chicago, 835 S Wolcott Ave, Chicago, IL 60612, USA
[c] Department of Microbiology and Immunology, University of Illinois at Chicago, 835 S. Wolcott Ave, Chicago, IL 60612, USA
[d] Department of Medicinal Chemistry and Pharmacognosy, University of Illinois at Chicago, 900 S. Ashland Ave, Chicago, IL 60607, USA
[e] Biophysics Core, Research Resources Center, University of Illinois at Chicago, 1100 S. Ashland Ave, Chicago, IL 60607, USA

ARTICLE INFO

Keywords:
Adenovirus
E3-19K
HLA-A2
Protein-protein interactions
Small molecule inhibitors
Molecular dynamic simulations
Molecular mechanics/generalized-born surface area (MM/GBSA)
Computational solvent mapping
Virtual screening
Surface plasmon resonance

ABSTRACT

The binding of the adenovirus (Ad) protein E3-19K with the human leukocyte antigen (HLA) plays an important role in Ad infections, which is the causative agent of a series of gastrointestinal, respiratory and ocular diseases. The objective of this research is to evaluate the essential interactions between E3-19K and HLA-A2 using the X-ray crystal structure of the E3-19K/HLA-A2 complex, and to identify small molecules that could potentially disrupt their binding. Computational methods, including molecular dynamic simulations, MM/GBSA calculations, and computational solvent mapping, were implemented to determine potential binding site(s) for small molecules. The previous experimentally determined hot spot residues, Q54 and E177 in HLA-A2, were also predicted to be the dominant residues for binding to E3-19K by our theoretical calculations. Several other residues were also found to play pivotal roles for the binding of E3-19K with HLA-A2. Residues adjacent to E177, including Q54 and several other residues theoretically predicted to be crucial in HLA-A2 were selected as a potential binding pocket to perform virtual screening with 1200 compounds from the Prestwick library. Seven hits were validated by surface plasmon resonance (SPR) as binders to HLA-A2 as a first step in identifying molecules that can perturb its association with the Ad E3-19K protein.

Adenovirus (Ad) infections are generally not a major concern in healthy individuals, but they can be severe and sometimes even fatal in children and immunocompromised adults.[1–3] More than 70 known serotypes for Ad (Ad1 ~ Ad70) have been reported, that are further classified into seven species from A to G.[4–8] In the 1980s, it was determined that the Ad protein E3-19K binds to the major histocompatibility complex (MHC) class I molecules, retaining them in the endoplasmic reticulum of the Ad infected cells, thereby blocking their escape to the surface of the cell.[9–11] By subverting the antigen-presenting function of the MHC class I molecules, the virus renders infected cells less susceptible to lysis by cytotoxic T-lymphocytes (CTLs).[12,13] A subsequent *in vivo* study with cotton rats confirmed a key role for E3-19K in Ad infections.[14] Human MHC class I molecules, known as human leukocyte antigen (HLA), are involved in distinguishing between "self" versus "foreign" proteins in the body. The importance of E3-19K in Ad infection in human cells suggests that disruption of E3-19K binding to MHC I could sensitize Ad-infected cells to lysis by CTLs. In this study, we evaluated the protein-protein interaction (PPI) of the E3-19K/HLA-A2 complex to identify a site where bound small molecule could inhibit PPI in order to discover potential inhibitors.

The crystal structure of the Ad2 E3-19K/HLA-A2 complex was determined by Li et al,[15] providing crucial information to explore potential binding sites for small molecules. The binding interface for the Ad2 E3-19K/HLA-A2 complex features two salt bridge interactions between K27 (Ad2 E3-19K) and E53 (HLA-A2), and K42 (Ad2 E3-19K) and E177 (HLA-A2). Additionally, hydrogen bond networks between A19, Y49, I51, Y88, Q92, Y93 of Ad2 E319K and D238, T178, E177, E69, K19, and S20 of HLAA2, respectively, also stabilize their interactions. Moreover, a number of hydrophobic contacts contribute to this PPI. However, from a visual analysis of static interactions alone, it is difficult to determine which contacts are pivotal for PPI and which ones act as energetically hot spots. Thus, we further explored the interactions

* Corresponding author at: Center for Biomolecular Sciences, University of Illinois at Chicago, 900 S. Ashland Ave, Chicago, IL 60607, USA.
E-mail address: mjohnson@uic.edu (M.E. Johnson).
[1] JR and NRD contributed equally to this work.

https://doi.org/10.1016/j.bmcl.2018.07.036
Received 6 July 2018; Received in revised form 24 July 2018; Accepted 26 July 2018
Available online 29 July 2018
0960-894X/

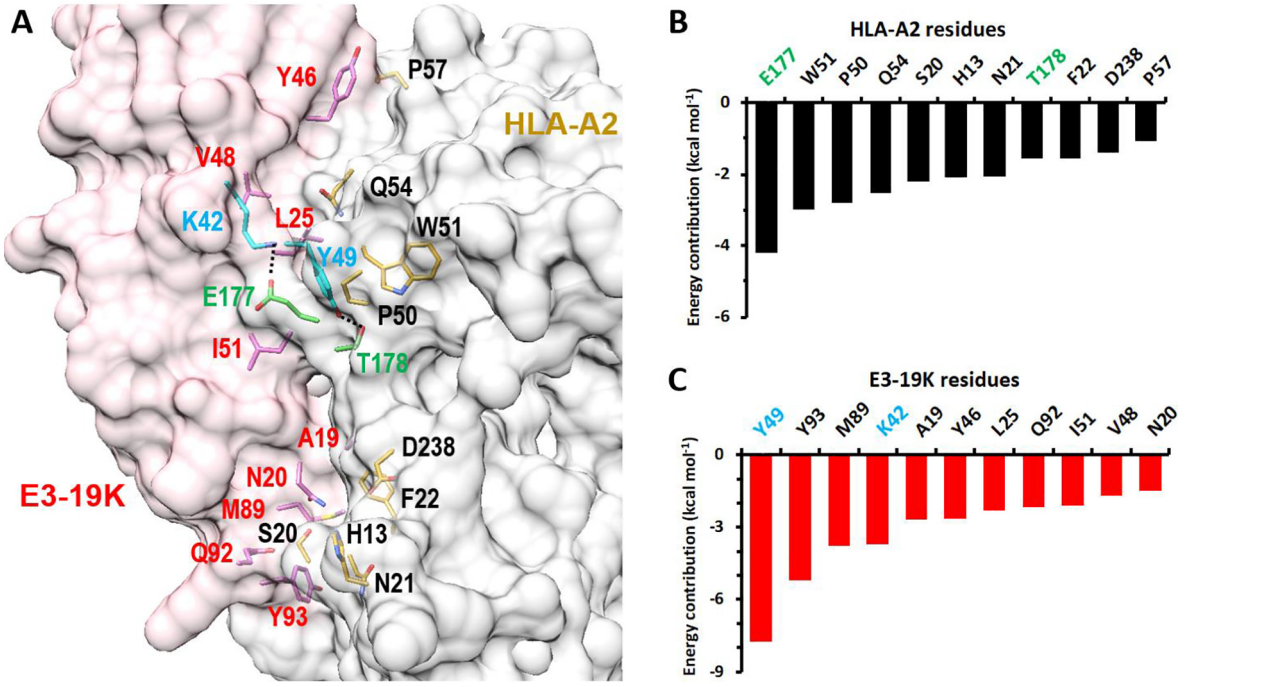

Fig. 1. The major residues for the Ad2 E3-19K/HLA-A2 complex that contribute to binding. (A) Principal contributing residues for HLA-A2 are shown with gold sidechains and are labelled in black, while favourable residues for Ad2 E3-19K are shown with hot pink sidechains and labelled in red. The surfaces of HLA-A2 and Ad2 E3-19K are in light gray and light pink respectively. The side chains contributing the two highest interaction energies, E177-K42 and Y49-T178, are highlighted in green and cyan for HLA-A2 and Ad2, respectively. Hydrogen bonds are shown as black dashed lines. The picture was prepared with Chimera1.10.2.[20] (B) Per-residue energetic contributions for the pivotal residues of HLA-A2; (C) Per-residue energetic contributions for the important residues of Ad2 E3-19K. Individual contributions for residues with energy contribution greater than 1 kcal mol^{-1} are listed.

by computational methods, including molecular dynamic (MD) simulations, molecular mechanics/generalized-born surface area (MM/GBSA) calculations and computational solvent mapping (CSM),[16] resulting in the identification of a most probable binding site. Since there is no known compound that inhibits this PPI, ligand-based approaches were not viable for identifying potential inhibitors, thus the Prestwick library was used to conduct virtual screening toward the promising binding site to identify potential binding compounds. The predicted binders were subjected to surface plasma resonance (SPR) to test their affinities with HLA-A2, and to evaluate the feasibility of developing small molecule inhibitors by disturbing the interaction between E3-19K and HLA-A2.

20-ns MD simulations of Ad2 E3-19K/HLA-A2 complex were initially performed in a water box, and per-residue energy decomposition was calculated to gain further insights into the energetic contributions of individual residues to the complex formation using the MM/GBSA approach.[17] Unsurprisingly, the most favorable residue interactions are distributed throughout the interface of the Ad2 E3-19K/HLA-A2 complex (Fig. 1A). The energetically most favorable interactions are formed by residues E177, W51, P50, Q54, S20, H13, N21, T178, F22, D238, and P57 from HLA-A2 (Fig. 1B) with Y49, Y93, M89, K42, A19, Y46, L25, Q92, I51, V48, and N20 from Ad2 E3-19K (Fig. 1C). It is notable that the dominant contributions of E177 in HLA-A2 and Y49 in Ad2 E3-19K reflect their critical roles in salt bridge and hydrogen bond interactions formed with their counterpart residues of K42 in Ad2 E3-19K and T178 of HLA-A2. Moreover, hydrogen bond interactions between the backbone carbonyl of D238 in HLA-A2 and the backbone NH of A19 in E3-19K, the S20 backbone in HLA-A2 and the Y93 sidechain in E3-19K, and the sidechain of E177 and backbone of I51 also contribute prominently to the binding. However, the two salt bridge interactions between Ad2 E3-19K and HLA-A2 show markedly different effects in stabilizing the PPI. The salt bridge formed by E177 of HLA-A2 and K42 of Ad2 E3-19K shows a dominant contribution to the binding, consistent with the experimental results of the E177K HLA-A2 mutant abolishing binding activity.[18,19] However, the salt bridge interaction formed by E53 of HLA-A2 with K27 of Ad2 E3-19K is unstable during MD simulations, with both residues contributing less than 1 kcal mol^{-1} for their binding (data not shown). Another residue tested through experimental mutant assay is Q54 of HLA-A2; the Q54G mutant significantly reduced to the binding affinity with Ad2 E3-19K.[19] It is notable that although Q54 contributes significantly to binding based on the theoretical energy decomposition, it contributes much less than that of E177 in HLA-A2, consistent with the experimental results of the E177K mutant abolishing activity while the Q54G mutant just reduces activity in HLA-A2. Therefore, the energy decomposition indicates that the dominant hot spots are E177 (HLA-A2) with K42 (Ad2 E3-19K) and Y49 (Ad2 E3-19K) with T178 (HLA-A2), suggesting that the surrounding area could be a viable binding site for small molecules.

Subsequently, we used an alternate approach, CSM, to explore the interface region, around the energetic hot spots for small molecule binding pockets. However, due to the sensitivity of CSM to conformational changes[21] the Multiscale Modeling Tools for Structural Biology (MMTSB)[22] were first utilized to identify the major conformations for the Ad2 E3-19K/HLA-A2 complex. The clustering analysis is presented in Fig. 2 with 4 different clusters identified using an RMSD radius of 1.5 Å during the 20-ns MD simulations. Cluster 1 was the dominant conformation, sampled for 50% of the simulation time. Clusters 2 and 3 occupied 22% and 18% of the simulation time, respectively. Cluster 2 was sampled during the last 5-ns of the simulations, while cluster 4 was only observed at the beginning of the simulation and occupied 10% of the conformation populations. One cluster centroid was picked from each cluster, and these four complexes were separated into the respective Ad2 E3-19K and HLA-A2 interface regions for the subsequent CSM analysis.

The FTMap online server applies the CSM method to probe small molecule binding sites. The four representative cluster structures of Ad2 E3-19K and the corresponding four HLA-A2 structures from the above MMTSB clustering were individually submitted to this server.[23] The

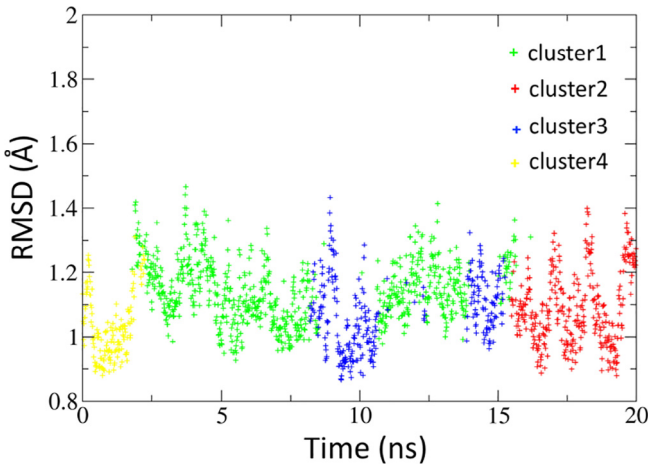

Fig. 2. Clustering distribution of the Ad2 E3-19K/HLA-A2 complex during the 20-ns MD simulations. Y-axis values represent the RMSD of individual snapshot structures from the centroid of the respective cluster.

mask strategy was used to focus on the PPI binding interface instead of searching the full protein surfaces. The output results generated by FTMap were in PDB format with consensus clusters of the different probes mapped to the surface of the Ad2 E3-19K or HLA-A2. Druggable binding sites are shown in Fig. 3 for consensus cluster strength above 16 and additional hot spots within 8 Å (weaker binding sites are not shown).[24,25] Several strong druggable binding sites were identified on Ad2 E3-19K and HLA-A2, respectively, by analyzing the consensus clusters of the probe molecules. There are four, three, two and two possible druggable binding sites (or consensus sites, *CS*) on the PPI interface of Ad2 E3-19K in the MMTSB cluster 1, cluster 2, cluster 3 and cluster 4, as shown in Fig. 3A–D, respectively. Two binding sites are commonly found in all of them and are circled in dark red dash lines. These two spots are primarily comprised of K42, A47, Y49 and K16, T23, L25, and are thus the FTMap predicted hot spots for Ad2 E3-19K. The results are consistent with the MM/GBSA per-residue contribution calculations above, since L25, K42 and Y49 are significant contributing residues for the interaction with HLA-A2 in the binding free energy calculation. Similarly, two hot spots were detected on the PPI interface of HLA-A2. One includes P50, W51, Q54, E177 and T178, while the other includes R12, H13, S20 and N21. These residues correspond to nearly all of those exhibiting contributions to HLA-A2 in the MM/GBSA decomposition (Fig. 1B).

MM/GBSA[26,27] and FTMap both identify the same residues as contributing to the HLA-A2/E3-19K interface stabilization. Accordingly, we used this information to determine the docking pocket most likely to provide an anchor for binding compounds that can interrupt the PPI binding. Conventional drug therapies against viruses mainly target viral enzymes, but a major drawback for this strategy is the high frequency emergence of resistant strains resulting from continuous mutation.[28,29] The alternative development of host-targeting inhibitors could dramatically enlarge the repertoire of therapeutic targets, and potentially offers a greater barrier to the emergence of resistance. Furthermore, targeting host molecules has the potential for broad-spectrum indications when targeting pathways are shared by the different variants of a given virus or by different types of virus.[30,31] Consequently, targeting HLA-A2 appears more promising, since so many serotypes of Ad have already been identified. Moreover, the experimental results indicate that the Q54G mutant of HLA-A2 interacts weakly with E3-19K, and that mutation of E177K on HLA-A2 abolishes the interactions with E3-19K, indicating that the interface is quite sensitive to relatively small structural alterations.[18,19] Consequently, we have focused on targeting either of the two druggable HLA-A2 *CS* that include P50, W51, Q54, E177 and T178. Subsequently, virtual screening using GOLD5.2.2[32] against HLA-A2 with the 1200 compound Prestwick chemical library was performed to identify novel scaffolds that bind to the hot spots. The binding site sphere was defined as being within 10 Å around the hot spot residue of E177, thus the residues of P50, W51, E53, Q54, L172, E173, N174, G175, K176, E177, T178, L179, Q180 are involved in the

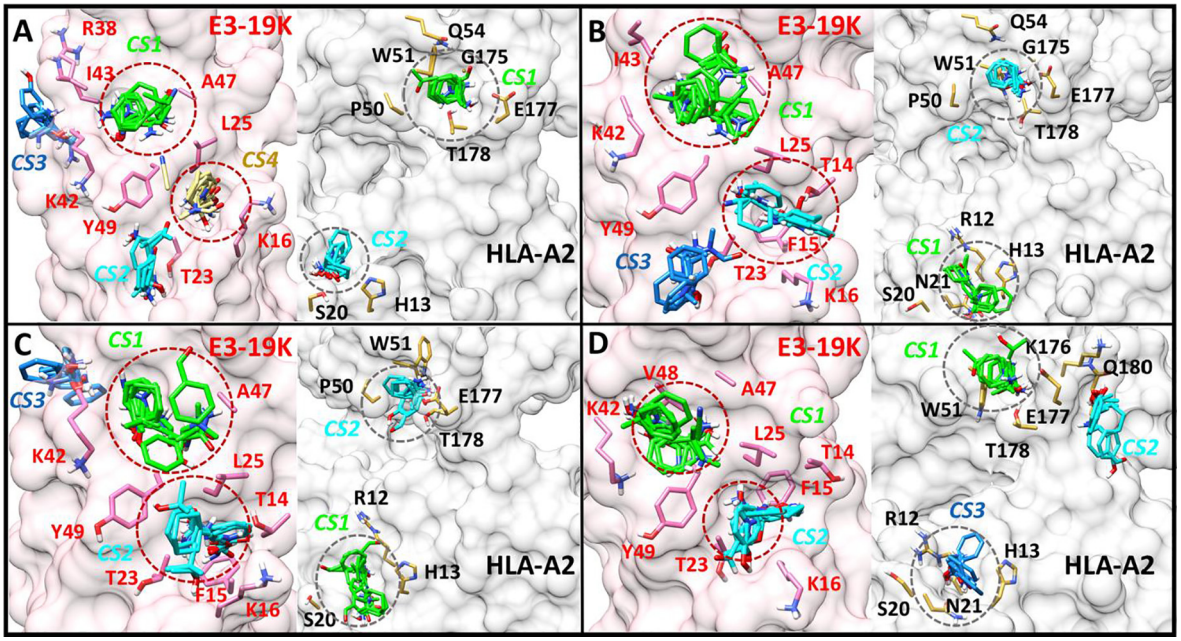

Fig. 3. FTMap druggable binding sites on Ad2 E3-19K and HLA-A2 for the MD simulations cluster 1 (A), cluster 2 (B), cluster 3 (C) and cluster 4 (D). Cluster 1 is the dominant conformation in MD simulations with population nearly 50% during 20-ns simulations. *CS1-CS4* are druggable consensus sites that could bind more than 16 probes in FTMap and they are named in order of their significance. *CS1* is the most important druggable binding site from FTMap, and is shown in green, *CS2* is the second most important, and colored in cyan, *CS3* ranks third and is colored in dodger blue, while *CS4* is the least important, and is shown in khaki. Ad2 E3-19K is shown in a light pink transparent surface with residues contributing to binding in pink sidechains. HLA-A2 is shown with a light gray transparent surface throughout, with pivotal residues shown with gold sidechains. The dark red and gray dashed circles are consensus druggable binding sites that occur in all four MMTSB clusters for Ad2 E3-19K and HLA-A2, respectively.

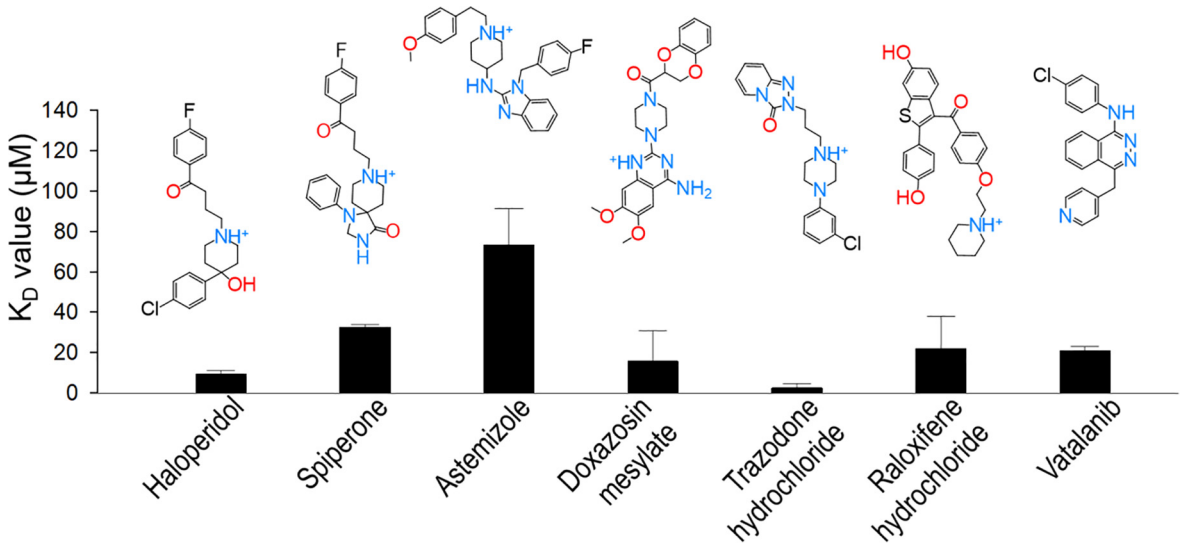

Fig. 4. Direct binding analysis by SPR. Binding affinities (K_D values) of seven hits to the immobilized HLA-A2 proteins were determined by fitting the SPR data with steady-state affinity model.

binding pocket. This includes the residues P50, W51, Q54, E177, and T178 that showed the highest contribution to the energy decomposition, as well as being one of the two identified hot spots. Compound selection was based on the ChemPLP[33] scoring function. The top 36 compounds according to ChemPLP were selected for experimental testing by SPR binding analysis to determine which ones were at least capable of binding to HLA-A2. Of 36 tested compounds, seven compounds directly bound to HLA-A2 with K_D values ranging from 2.5 μM to 75 μM. All seven compound structures and K_D values are illustrated in Fig. 4. Two compounds, Haloperidol and Trazodone hydrochloride, had tighter interaction, with K_D values below 10 μM and Trazodone showed the best binding affinity with K_D values at 2.5 ± 2.2 μM. Three compounds (Doxazosin, Raloxifene, and Vatalanib) showed moderate binding affinities at 15.7 μM, 22.0 μM, and 21.2 μM, respectively, while Astemizole showed the lowest affinity.

Fig. 5 shows the docking poses of two representative compounds, Astemizole and Trazodone. The NH^+ group in the six-member ring contained in both compounds interacts with hot spot residue E177 in HLA-A2 by salt bridge interactions, mimicking the interaction of the K42 sidechain in Ad2 E3-19K. Additionally, one hydrogen bond interaction was found between Astemizole and the sidechain of T178, that also mimics the interaction with Y49 in Ad2 E3-19K. Moreover, the aromatic rings of the compounds exhibit stacking interactions with the amide moiety of Q54 and the indole moiety of W51, as well as hydrophobic interactions that also promote their binding.

In conclusion, 20-ns MD simulations were performed on the crystal complex of Ad2 E3-19K/HLA-A2 in a water environment, and energy decompositions were calculated to predict the hot spots by MM/GBSA per-residue decomposition. Q54 in HLA-A2 contributes significantly to the energy decomposition, although much less than that of the hot spot residue E177. This result is consistent with the experimental results of Q54G reducing the activity rather than abolishing it as E177K did. The FTMap results also confirm the hot spot and binding area for small molecules from MM/GBSA. The theoretical predictions help explain the experimental results and provide more extensive information on the binding of Ad2 E3-19K and HLA-A2. Considering the emergence of resistant strains of the virus, a host-targeting strategy was applied in this research to explore the potential for broad-spectrum inhibitors by selecting HLA-A2 as a target. Then, a virtual screening with GOLD was performed on HLA-A2 with 1200 compounds from the Prestwick library within the binding area determined by MM/GBSA and FTMap. The top 36 compounds with the highest ChemPLP scores were selected to experimentally investigate their binding affinities with HLA-A2. Seven hits were validated by SPR as binding to HLA-A2 at the micromolar level. To our knowledge, this is the first approach to discover small molecule inhibitors of adenovirus that potentially bind to the interface between Ad2 E3-19K and HLA-A2. Work is continuing to develop analogs of these compounds with improved potency and molecular properties.

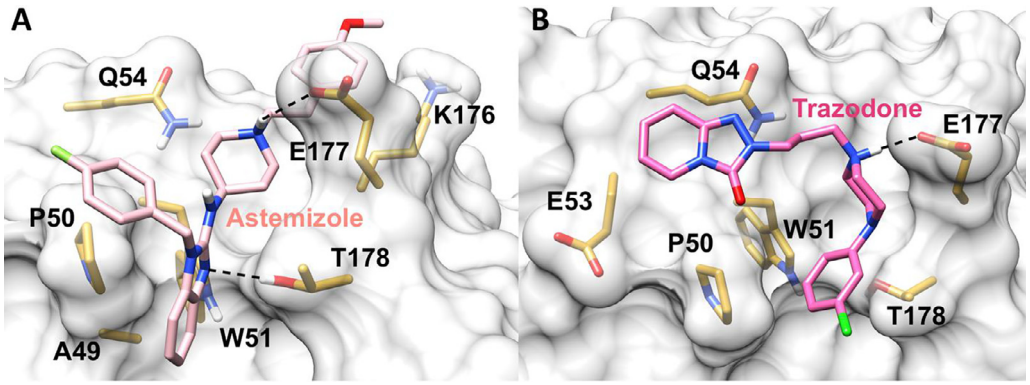

Fig. 5. Docking poses of Astemizole (A) and Trazodone (B) with HLA-A2. Interacting residues of HLA-A2 are colored in gold, salt bridge contacts are indicated by dashed lines and the surface of HLA-A2 is colored in light gray.

Acknowledgements

This work was supported in part by National Institutes of Health Grant R03 AI114611. The authors thank the UIC Academic Computing and Communications Center for access to the high-performance computing cluster, Extreme, to perform the computational work. We also thank ChemAxon for access to JChem for Excel, used for data management. Molecular graphics and analyses for Fig. 1, Fig. 3, and Fig. 5 utilized the UCSF Chimera package, which is developed by the Resource for Biocomputing, Visualization, and Informatics at the University of California, San Francisco (supported by NIGMS P41-GM103311).

Appendix A. Supplementary data

Supplementary data associated with this article can be found, in the online version, at https://doi.org/10.1016/j.bmcl.2018.07.036.

References

[1]. Flomenberg P, Babbitt J, Drobyski WR, et al. Increasing incidence of adenovirus disease in bone-marrow transplant recipients. *J Infect Dis.* 1994;169(4):775–781.
[2]. Kosulin K, Geiger E, Vecsei A, et al. Persistence and reactivation of human adenoviruses in the gastrointestinal tract. *Clin Microbiol Infect.* 2016;22(4)..
[3]. Lion T, Kosulin K, Geiger E, et al. Persistence and reactivation of human adenoviruses in the immunocompromised host. *Pediatr Blood Cancer.* 2015;62:S146.
[4]. Hage E, Dhingra A, Liebert UG, Bergs S, Ganzenmueller T, Heim A. Three novel, multiple recombinant types of species of human mastadenovirus D (HAdV-D 73, 74 & 75) isolated from diarrhoeal faeces of immunocompromised patients. *J Gen Virol.* 2017;98(12):3037–3045.
[5]. Hage E, Liebert UG, Bergs S, Ganzenmueller T, Heim A. Human mastadenovirus type 70: a novel, multiple recombinant species D mastadenovirus isolated from diarrhoeal faeces of a haematopoietic stem cell transplantation recipient. *J Gen Virol.* 2015;96:2734–2742.
[6]. Hiroi S, Morikawa S, Takahashi K, Komano J, Kase T. Molecular epidemiology of human adenoviruses D associated with epidemic keratoconjunctivitis in Osaka, Japan, 2001–2010. *Jpn J Infect Dis.* 2013;66(5):436–438.
[7]. Li YM, Zhou WM, Zhao YJ, et al. Molecular, Typing and epidemiology profiles of human adenovirus infection among paediatric patients with severe acute respiratory infection in China. *Plos One.* 2015;10(4).
[8]. Wadell G. Molecular epidemiology of human adenoviruses. *Curr Top Microbiol.* 1984;110:191–220.
[9]. Andersson M, Paabo S, Nilsson T, Peterson PA. Impaired intracellular-transport of class-I Mhc antigens as a possible means for adenoviruses to evade immune surveillance. *Cell.* 1985;43(1):215–222.
[10]. Burgert HG, Kvist S. An adenovirus type-2 glycoprotein blocks cell-surface expression of human histocompatibility class-I antigens. *Cell.* 1985;41(3):987–997.
[11]. Kvist S, Ostberg L, Persson H, Philipson L, Peterson PA. Molecular association between transplantation antigens and cell-surface antigen in adenovirus-transformed cell line. *Proc Natl Acad Sci USA.* 1978;75(11):5674–5678.
[12]. Andersson M, Mcmichael A, Peterson PA. Reduced allorecognition of adenovirus-2 infected-cells. *J Immunol.* 1987;138(11):3960–3966.
[13]. Flomenberg P, Piaskowski V, Truitt RL, Casper JT. Human adenovirus-specific CD8(+) T-cell responses are not inhibited by E3–19K in the presence of gamma interferon. *J Virol.* 1996;70(9):6314–6322.
[14]. Ginsberg HS, Lundholmbeauchamp U, Horswood RL, et al. Role of early region-3 (E3) in pathogenesis of adenovirus disease. *Proc Natl Acad Sci USA.* 1989;86(10):3823–3827.
[15]. Li LN, Muzahim Y, Bouvier M. Crystal structure of adenovirus E3–19K bound to HLA-A2 reveals mechanism for immunomodulation. *Nat Struct Mol Biol.* 2012;19(11) 1176-+.
[16]. Dennis S, Kortvelyesi T, Vajda S. Computational mapping identifies the binding sites of organic solvents on proteins. *Proc Natl Acad Sci.* 2002;99(7):4290.
[17]. Tsui V, Case DA. Theory and applications of the generalized Born solvation model in macromolecular simulations. *Biopolymers.* 2001;56(4):275–291.
[18]. Fu J, Li L, Bouvier M. Adenovirus E3–19K proteins of different serotypes and subgroups have similar, yet distinct, immunomodulatory functions toward major histocompatibility class I molecules. *J Biol Chem.* 2011;286(20):17631–17639.
[19]. Li L, Santarsiero BD, Bouvier M. Structure of the adenovirus type 4 (Species E) E3–19K/HLA-A2 complex reveals species-specific features in MHC class I recognition. *J Immunol.* 2016;197(4):1399.
[20]. Pettersen EF, Goddard TD, Huang CC, et al. UCSF Chimeraavisualization system for exploratory research and analysis. *J Comput Chem.* 2004;25(13):1605–1612.
[21]. Lexa KW, Carlson HA. Full protein flexibility is essential for proper hot-spot mapping. *J Am Chem Soc.* 2011;133(2):200–202.
[22]. Feig M, Karanicolas J, Brooks CL. MMTSB Tool Set: enhanced sampling and multiscale modeling methods for applications in structural biology. *J Mol Graph Model.* 2004;22(5):377–395.
[23]. Ngan CH, Bohnuud T, Mottarella SE, et al. FTMAP: extended protein mapping with user-selected probe molecules. Nucleic Acids Research. 2012;40(Web Server issue): W271-W275.
[24]. Kozakov D, Hall DR, Chuang GY, et al. Structural conservation of druggable hot spots in protein-protein interfaces. *Proc Natl Acad Sci USA.* 2011;108(33):13528–13533.
[25]. Kozakov D, Grove LE, Hall DR, et al. The FTMap family of web servers for determining and characterizing ligand-binding hot spots of proteins. *Nat Protocols.* 2015;10:733.
[26]. Ren J, Mistry TL, Su P-C, et al. Determination of absolute configuration and binding efficacy of benzimidazole-based FabI inhibitors through the support of electronic circular dichroism and MM-GBSA techniques. *Bioorg Med Chem Lett.* 2018;28(11):2074–2079.
[27]. Rastelli G, Rio AD, Degliesposti G, Sgobba M. Fast and accurate predictions of binding free energies using MM-PBSA and MM-GBSA. *J Comput Chem.* 2010;31(4):797–810.
[28]. van der Vries E, Schutten M, Fraaij P, Boucher C, Osterhaus A. Chapter six – influenza virus resistance to antiviral therapy. In: De Clercq E, ed. *Advances in Pharmacology.* Vol 67. Academic Press; 2013:217–246.
[29]. Kieffer TL, George S. Resistance to hepatitis C virus protease inhibitors. *Curr Opin Virol.* 2014;8:16–21.
[30]. Prussia A, Thepchatri P, Snyder JP, Plemper RK. Systematic approaches towards the development of host-directed antiviral therapeutics. *Int J Mol Sci.* 2011;12(6):4027–4052.
[31]. de Chassey B, Meyniel-Schicklin L, Vonderscher J, André P, Lotteau V. Virus-host interactomics: new insights and opportunities for antiviral drug discovery. *Genome Med.* 2014;6(11):115.
[32]. Verdonk ML, Cole JC, Hartshorn MJ, Murray CW, Taylor RD. Improved protein–ligand docking using GOLD. *Proteins: Struct Funct Bioinf.* 2003;52(4):609–623.
[33]. Korb O, Stützle T, Exner TE. Empirical Scoring Functions for advanced protein – ligand docking with PLANTS. *J Chem Inf Model.* 2009;49(1):84–96.